Expression and purification of a recombinant amyloidogenic peptide from transthyretin for solid-state NMR spectroscopy

Philippe S. Nadaud [a,1], Mohosin Sarkar [a,1], Bo Wu [a], Cait E. MacPhee [b], Thomas J. Magliery [a,c], Christopher P. Jaroniec [a,*]

[a] Department of Chemistry, The Ohio State University, Columbus, OH 43210, USA
[b] SUPA, School of Physics and Astronomy, The University of Edinburgh, Edinburgh EH9 3JZ, UK
[c] Department of Biochemistry, The Ohio State University, Columbus, OH 43210, USA

ARTICLE INFO

ABSTRACT

We describe the expression and purification of a model amyloidogenic peptide comprising residues 105–115 of human transthyretin (TTR105–115). Recombinant TTR105–115, which does not contain any non-native residues, was prepared as part of a fusion protein construct with a highly soluble B1 immunoglobulin binding domain of protein G (GB1), with typical yields of ∼4 mg/L of uniformly $^{13}C,^{15}N$-enriched HPLC-purified peptide per liter of minimal media culture. Amyloid fibrils formed by recombinant TTR105–115 were characterized by transmission electron microscopy and solid-state NMR spectroscopy, and found to be comparable to synthetic TTR105–115 fibrils. These results establish recombinant TTR105–115 as a valuable model system for the development of new solid-state NMR techniques for the atomic-level characterization of amyloid architecture.

© 2009 Elsevier Inc. All rights reserved.

Introduction

Amyloid fibrils are highly ordered filamentous aggregates formed by the self-assembly of polypeptide molecules that, in their soluble forms, display a variety of structures and functions [1]. Amyloid formation has long been implicated in the development of multiple neurodegenerative and systemic protein misfolding disorders in humans, including Alzheimer's and Parkinson's diseases and type II diabetes [2–4]. Moreover, the fact that numerous peptides and proteins not associated with any recognized disease can also be converted to fibrils under denaturing conditions [5,6], has led to the suggestion that the amyloid conformation represents an alternative, stable structural state of all polypeptide chains [3,4]. Indeed, the remarkable ability of many peptide sequences to readily self-assemble into ordered amyloid structures has been recently found to play useful biological roles [7], and has also been exploited to design novel nanomaterials with unique physical properties and biological functions [8–10].

The detailed characterization of amyloid structures is currently an area of intense research. Extensive experimental data afforded by relatively low-resolution imaging techniques, including transmission electron microscopy (TEM),[2] atomic force microscopy, and X-ray fiber diffraction, reveal that fibrils derived from different polypeptide precursors exhibit several common features [1–4]. These include unbranched morphologies characterized by lengths in the μm regime and diameters of ∼10 nm, and supramolecular architectures consisting of a small number of protofilaments coiled around the long axis of the fibril. The protofilaments themselves contain a relatively rigid core region typically made up of several β-sheets running parallel to the fibril axis, with the individual peptide strands oriented perpendicular to this axis. More recently, major advances have also been made in interrogating the molecular structures of amyloid peptides and proteins with atomic-resolution using X-ray microcrystallography [11–13] and solid-state nuclear magnetic resonance (SSNMR) spectroscopy [14–33].

To date, the vast majority of SSNMR studies of amyloidogenic peptides have been carried out by using samples prepared via solid-phase peptide synthesis (SPPS) with selective ^{13}C and/or ^{15}N amino acid labeling [14–24]. The obvious advantage of this approach is that it yields NMR spectra that are relatively straightforward to

---

* Corresponding author. Address: Department of Chemistry, The Ohio State University, 1035 Evans Laboratory, 100 West 18th Avenue, Columbus, OH 43210, USA. Fax: +1 614 292 1685.
E-mail address: jaroniec@chemistry.ohio-state.edu (C.P. Jaroniec).
[1] These authors contributed equally to this work.

[2] *Abbreviations used:* TEM, transmission electron microscopy; SPPS, solid-phase peptide synthesis; IPTG, isopropyl β-ᴅ-thiogalactoside; PMSF, phenylmethanesulphonylfluoride; HSQC, heteronuclear single quantum coherence; GB1, B1 immunoglobulin binding domain of protein G; TFA, trifluoroacetic acid; DSS, 2, 2-dimethylsilapentane-5-sulfonic acid.

interpret. At the same time, comprehensive SSNMR structural studies of amyloid fibrils based on such selective labeling schemes are generally highly labor-intensive, requiring the preparation of many peptide samples. Another potential disadvantage of the selective labeling approach is the additional synthetic effort or prohibitive cost associated with obtaining certain ^{13}C,^{15}N-labeled amino acid precursors required for SPPS. While for certain systems selective isotope labeling remains effectively the only viable approach for obtaining site-specific structural information, many amyloid peptides exhibit SSNMR spectra of quality that is sufficient to make them amenable to detailed structural studies by using one or few highly or uniformly ^{13}C,^{15}N (U–^{13}C,^{15}N) enriched samples in combination with multidimensional SSNMR techniques. Indeed, the recent advances in biomolecular SSNMR methodology, demonstrated widely for microcrystalline peptides and proteins [34–37], have already enabled studies of amyloid fibrils formed by several U–^{13}C,^{15}N-labeled polypeptides prepared by recombinant DNA techniques [27–33].

The availability of small amyloidogenic peptides that can be readily prepared by expression in *Escherichia coli* in a variety of ^{13}C and ^{15}N labeling schemes (e.g., U–^{13}C,^{15}N or uniform ^{15}N and sparse ^{13}C enrichment by using 1,3-^{13}C-glycerol or 2-^{13}C-glycerol based expression media [38]), and that can serve as model systems for the development of new SSNMR methodologies for atomic-level studies of amyloid architecture, is highly desirable. However, with several notable exceptions [39–48], the preparation of recombinant amyloid peptides of this type has been hampered by their toxicity and propensity to aggregate. Here we describe the expression and purification of one particularly valuable model amyloidogenic peptide, corresponding to residues 105–115 of human transthyretin (TTR105–115), which readily and reproducibly forms homogeneous amyloid fibrils [49] that yield highly-resolved SSNMR spectra [17]—in fact, these favorable spectroscopic properties have recently facilitated the determination of an atomic-resolution structure of TTR105–115 in the fibrillar state [18]. Notably, the recombinant TTR105–115 peptide in the present study was prepared as part of a fusion protein construct by using relatively straightforward procedures analogous to those typically employed for the expression of soluble non-amyloidogenic peptides [50–53]. Specifically, the highly soluble B1 immunoglobulin binding domain of protein G (GB1) [52–57], containing an additional N-terminal 6× His-tag, was used within a pET11a-based system as the fusion partner for TTR105–115. The His$_6$-GB1-TTR105–115 protein construct also contained a specific Factor Xa cleavage site prior to the TTR105–115 sequence [52], which enabled the recovery of the target peptide containing no N-terminal modifications. Following protein expression, purification and cleavage, the TTR105–115 peptide was purified by reverse-phase HPLC. The resulting recombinant peptide displays solution-state NMR spectra that are nearly identical to those obtained for a control sample prepared by SPPS. Moreover, it forms homogeneous amyloid fibrils as assessed by electron microscopy. This is further supported by the highly-resolved 1D and 2D SSNMR spectra obtained for U–^{13}C,^{15}N enriched TTR105–115 fibrils, which display ^{13}C chemical shifts consistent with those reported previously for selectively labeled synthetic fibrils [17,18].

Materials and methods

Plasmid construction

TTR105–115 was fused to the C-terminus of the T2Q mutant of GB1 (referred to as GB1 throughout the paper) with a short linker sequence and specific protease (Factor Xa) cleavage site in between (Fig. 1). A 6× His-tag was introduced at the N-terminus of GB1 for
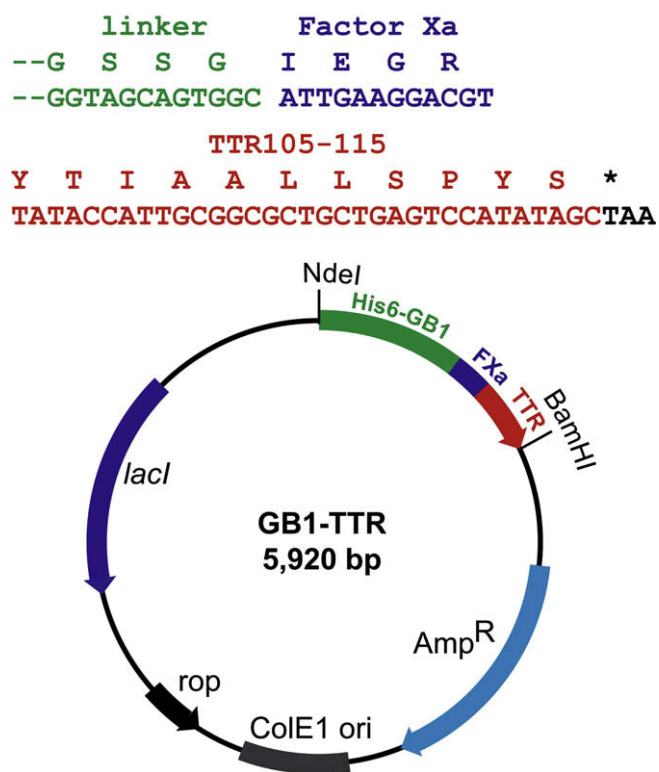

Fig. 1. Schematic representation of the GB1-TTR expression vector. Sequences for the linker, Factor Xa cleavage site and TTR105–115 peptide are indicated.

Ni^{2+} affinity purification. The gene encoding for GB1 was PCR amplified from a pET11a-based GB1 plasmid (kindly provided by Dr. Angela Gronenborn) using the following forward (5′–AATAAT AATCATATGGGACATCATCATCACCACCACGGCAGCAGCGGCACTTAC AGCTTATCCTGAACG–3′) and reverse (5′–AATAATGGATCCTTAG CTATATGGACTCAGCAGCGCCGCAATGGTATAACGTCCTTCAATGCCA CTGCTACCCTCGGTTACCGTGAAGGTTTTG–3′) primers. The forward primer was designed to contain a NdeI restriction site and 6× His sequence, and the reverse primer contained oligonucleotide sequences coding for a flexible four-residue (Gly-Ser-Ser-Gly) linker, Factor Xa cleavage site (Ile-Glu-Gly-Arg), TTR105–115 peptide (Tyr-Thr-Ile-Ala-Ala-Leu-Leu-Ser-Pro-Tyr-Ser) and BamHI restriction site. Both oligonucleotides were purchased from Sigma Genosys. Following digestion of the PCR product with NdeI and BamHI, the purified PCR product was ligated to obtain the final pET11a-His$_6$-GB1-TTR105–115 plasmid (termed GB1-TTR for brevity). The sequence of the inserted segment was confirmed by DNA sequencing (GENEWIZ, South Plainfield, NJ).

Expression of His$_6$-GB1-TTR105–115 fusion protein

The GB1-TTR plasmid was transformed into *E. coli* BL21(DE3) electrocompetent cells. For the expression of natural abundance protein, a 20 mL culture was grown overnight to saturation at 37 °C in Luria–Bertani (LB) medium containing ampicillin at a concentration of 100 μg/mL. One liter of fresh LB medium was subsequently inoculated with this 20 mL culture and grown at 30 °C until the culture reached an OD$_{600}$ of ∼0.75. Protein expression was induced by the addition of isopropyl β-ᴅ-thiogalactoside (IPTG) to a final concentration of 0.5 mM and the cell growth was continued at 30 °C for 10 h. For the expression of U–^{13}C,^{15}N-labeled protein, a 20 mL culture grown in LB medium as described

above was spun down and the pellet was resuspended in 1 L of modified M9 minimal medium containing 1 g/L $^{15}NH_4Cl$ and 2 g/ L ^{13}C-glucose as the sole nitrogen and carbon sources, respectively [58]. The remainder of the expression protocol was identical to that for natural abundance protein. Following protein expression cells were immediately chilled on ice and harvested by centrifugation at 4 °C and 7000 rpm using a Sorvall SLA-3000 rotor for 10 min. The cell pellets were either used immediately or stored at −80 °C until further use.

Purification of His₆-GB1-TTR105–115

The pellet from a 1 L cell culture was resuspended in 40 mL of lysis buffer (50 mM sodium phosphate, 100 mM NaCl, 10 mM imidazole, pH 8.0) containing 0.25 mg/mL lysozyme (Sigma), one protease inhibitor cocktail tablet (Roche), 5 μL of 10 mg/mL DNase solution, 20 μL of 10 mg/mL RNase solution, 0.1% Triton X-100, and 50 μL of 100 mM phenylmethanesulphonylfluoride (PMSF) solution, and incubated on ice for 1 h. For complete lysis the cells were subjected to sonication using a Misonix Sonicator 3000 with the following parameters: 30 s burst, 2 min interval, power level 7, repeated 6 times. The cell lysate was collected after centrifugation at 4 °C and 18,000 rpm using a Sorvall SS-34 rotor for 1 h and heated at 80 °C for 10 min. Insoluble material was removed by centrifugation for 1 h at 4 °C and 18,000 rpm. The clear cell lysate was then mixed with 2 mL of Ni–NTA agarose resin (Qiagen) equilibrated with the lysis buffer, gently shaken using a Nutator mixer for 2 h, and loaded onto a Bio-Rad disposable chromatography column. The column was washed twice with 15 mL of wash buffer (50 mM sodium phosphate, 100 mM NaCl, 0.1% Triton X-100, 20 mM imidazole, pH 8.0) and the His₆-GB1-TTR105–115 protein was eluted with 15 mL of elution buffer (50 mM sodium phosphate, 100 mM NaCl, 0.1% Triton X-100, 250 mM imidazole, pH 8.0).

Enzymatic digestion of His₆-GB1-TTR105–115

The His₆-GB1-TTR105–115 protein solution was concentrated to a volume of 5 mL using a 3000 molecular-weight-cut-off YMC Centriprep column (Millipore). The buffer was exchanged to 20 mM Tris·HCl, 50 mM NaCl, 2 mM CaCl₂, pH 7.2 using a PD10 column (GE Healthcare), and the protein was treated with Factor Xa protease (New England Biolabs) at 24 °C for 16 h using a protein-to-enzyme ratio of 1000:1 (w/w). The reaction was quenched by freezing the sample at −20 °C. Subsequently, 2 mL of Ni–NTA resin (equilibrated with 20 mM Tris·HCl, 50 mM NaCl, 2 mM CaCl₂, 0.1% Triton X-100, pH 7.2 buffer containing 5 mM imidazole) was added to the cleaved sample and mixed at 4 °C for 2 h with gentle shaking on a Nutator mixer. The mixture was applied to a disposable chromatography column and the flow-through containing TTR105–115 was collected and lyophilized.

HPLC purification of recombinant TTR105–115

Lyophilized TTR105–115 was dissolved in 2 mL of 1:1 (v/v) acetonitrile–water solution containing 0.1% (v/v) trifluoroacetic acid (TFA), filtered and subjected to purification by reverse-phase HPLC using a preparative C₁₈ column (Higgins Analytical, Inc.). The peptide was eluted with a linear acetonitrile gradient (3–90%) in water containing 0.1% TFA using a flow rate of 1 mL/min. Eluted fractions were monitored via UV absorbance at 280 nm and collected in a fraction collector in 4 mL aliquots. Fractions containing TTR105–115 were pooled together and lyophilized. The peptide identity and purity were confirmed by MALDI TOF mass spectrometry.

Solution-state NMR spectroscopy

Solution-state NMR spectra were recorded at 25 °C using a 600 MHz Bruker spectrometer equipped with a triple-resonance pulsed field gradient probe. Natural abundance and U–^{13}C,^{15}N-labeled recombinant TTR105–115, as well as an unlabeled TTR105–115 control sample prepared using Fmoc-SPPS purchased from CS Bio (Menlo Park, CA) were transferred to 5 mm sample tubes (Wilmad-Labglass, Buena, NJ) at concentrations of ~1 mM for the natural abundance peptides and ~4 mM for U–^{13}C,^{15}N-TTR105–115 in aqueous solution containing 20% acetonitrile-d_3 and 0.1% TFA. In addition to one-dimensional (1D) ^1H spectra, 2D ^1H–^1H TOCSY and ROESY spectra [59] were recorded for the natural abundance samples in order to confirm the previously published resonance assignments [60]. Moreover, to establish the extent of isotope labeling of recombinant U–^{13}C,^{15}N-TTR105–115, undecoupled and ^{15}N/^{13}C-decoupled 1D ^1H spectra, and ^{13}C-decoupled and $^{13}C'$-coupled 2D ^1H–^{15}N heteronuclear single quantum coherence (HSQC) spectra [59] were recorded. The 1D spectra were processed within the Bruker XWin-NMR software, and the 2D spectra were processed using the NMRPipe/NMRDraw software package [61] and analyzed using Sparky [62].

Amyloid fibril formation and electron microscopy

Lyophilized TTR105–115 was dissolved at a concentration of 10 mg/mL in an aqueous solution containing 10% (v/v) acetonitrile, 0.02% (w/v) sodium azide and adjusted to pH 2 with HCl. This solution was then incubated at 37 °C for 48 h, followed by incubation for 14 days at room temperature [17]. Amyloid fibril formation was typically observed within ~12 h, as evidenced by the appearance of a clear, viscous gel. For TEM measurements the fibrils were diluted to 1 mg/mL in water. A 5 μL aliquot was then deposited onto a 400 mesh Formvar/Carbon coated copper TEM grid purchased from Canemco (Quebec, Canada) and allowed to adsorb for 1 min. The sample was washed using three 10 μL aliquots of H_2O, with excess water removed using filter paper, and stained with 10 μL of 2% (w/v) uranyl acetate for 1 min. Amyloid fibrils were viewed using a FEI Technai G2 Spirit TEM with an accelerating voltage of 80 kV.

Solid-state NMR spectroscopy

Recombinant U–^{13}C,^{15}N-TTR105–115 amyloid fibrils were prepared as described above, centrifuged at 4 °C and 80,000 rpm using a Beckman-Coulter TLA-100.3 rotor for 2 h, washed thoroughly with ultrapure water, and centrifuged again for 2 h. The pellet containing the fibrils was then transferred to a 3.2 mm zirconia rotor purchased from Varian Inc. (Palo Alto, CA). Solid-state NMR experiments were performed on a three-channel Varian spectrometer operating at frequencies of 499.8 MHz for ^1H, 125.7 MHz for ^{13}C and 50.6 MHz for ^{15}N, and equipped with a 3.2 mm BioMAS probe [63]. The MAS frequency was regulated at 8929 ± 3 Hz, and the sample temperature was ~5 °C. Typical ^1H and ^{13}C 90° pulse lengths were 2.5 and 5 μs, respectively and during chemical shift evolution periods TPPM proton decoupling [64] was applied at a field strength of ~70 kHz. Additional experimental details are provided in the caption of Fig. 7. Spectra were processed using the NMRPipe/NMRDraw software package [61]. Chemical shifts were referenced relative to 2,2-dimethylsilapentane-5-sulfonic acid (DSS) with adamantane used as a secondary standard assuming the ^{13}C chemical shift of 40.48 ppm for the downfield resonance [65].

Results and discussion

Expression, purification and enzymatic digestion of His$_6$-GB1-TTR105–115

A schematic of the pET11a-based GB1-TTR expression vector, containing the TTR105–115 peptide fused to the C-terminus of GB1, is shown in Fig. 1. GB1 was employed as a fusion partner for TTR105–115 due to its high solubility, extremely stable three-dimensional fold characterized by an unusually high $T_m \sim 87\,°C$, and the fact that the wild-type (wt) protein can be overexpressed in *E. coli* at very high levels (typically in excess of 100 mg of protein per liter of cell culture) [66]. Indeed, these desirable characteristics have previously led to the use of GB1 within other fusion protein expression constructs [52–57]. To facilitate the rapid and efficient purification of GB1-TTR105–115 by Ni^{2+} affinity chromatography, an additional 6× His-tag was incorporated at the N-terminus of GB1. Moreover, in order to enable the isolation of unmodified TTR105–115 peptide, a flexible four-residue linker followed by a Factor Xa protease site was introduced between the C-terminus of GB1 and the TTR105–115 sequence [52].

Prior to the large scale expression of unlabeled and isotopically labeled His$_6$-GB1-TTR105–115 the temperature, IPTG concentration and length of the induction period were independently optimized (data not shown). Maximum protein yields—typically ~40 mg protein per liter of minimal media culture (see Table 1)—were obtained for expression at 30 °C for 9–12 h with 0.5 mM IPTG. Following protein expression and cell lysis two straightforward purification steps, comprising heat treatment of the lysate at 80 °C and elution through a Ni–NTA column, were used to yield His$_6$-GB1-TTR105–115 with greater than 95% purity as illustrated in lanes 2–4 of the SDS–PAGE gel in Fig. 2. The fusion protein was subsequently treated with Factor Xa protease to release the TTR105–115 peptide, and the reaction mixture was applied to a Ni–NTA resin to separate TTR105–115 from the other cleavage product, His$_6$-GB1, as well as any uncleaved His$_6$-GB1-TTR105–115 starting material—the TTR105–115 peptide was collected in the flow-through fraction and lyophilized, and the His-tagged proteins were eluted from the Ni–NTA column for further analysis. Although we were not able to directly visualize TTR105–115 using SDS–PAGE due to the low molecular weight of the peptide, the efficacy of the Factor Xa cleavage reaction and the subsequent Ni^{2+} affinity purification step could be assessed using this method by monitoring the various protein species present in the reaction mixture. Lanes 5 and 6 of the SDS–PAGE gel in Fig. 2 indicate that the Factor Xa digestion is highly efficient as judged by the small size of the band corresponding to uncleaved His$_6$-GB1-TTR105–115 relative to His$_6$-GB1. Moreover, the Ni–NTA resin treatment effectively separates both His-tagged protein species from the TTR105–115 peptide. We note here that in SDS–PAGE His$_6$-GB1 runs anomalously slowly compared to His$_6$-GB1-TTR105–115. This may be caused by residual structure of His$_6$-GB1 in SDS, perhaps resulting from its increased thermal stability compared to His$_6$-GB1-TTR105–115.
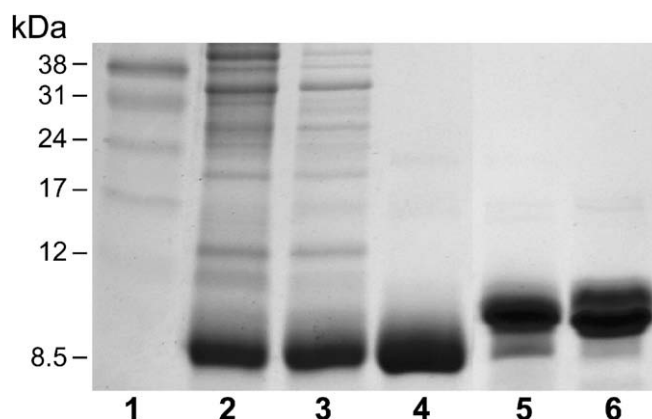

Fig. 2. Purification and Factor Xa digestion of His$_6$-GB1-TTR105–115 analyzed by SDS–PAGE using an 18% polyacrylamide gel. Protein samples were mixed in a 1:1 (v/v) ratio with a standard gel loading buffer containing 10 mM DTT and heated at 98 °C for 5 min prior to loading onto the gel. Lane 1: molecular weight marker (Low range rainbow marker, GE Healthcare); lane 2: total protein obtained by solubilizing pelleted whole cells in loading buffer; lane 3: cell lysate heated at 80 °C for 10 min; lane 4: Ni–NTA column eluate consisting primarily of His$_6$-GB1-TTR105–115 fusion protein; lane 5: His$_6$-GB1-TTR105–115 following Factor Xa treatment; lane 6: Ni–NTA column eluate from Factor Xa treated His$_6$-GB1-TTR105–115 (the flow-through fraction contains TTR105–115, not visualized by SDS–PAGE).

Purification of recombinant TTR105–115

The lyophilized TTR105–115 sample obtained from the Ni–NTA flow-through was dissolved in an aqueous acetonitrile solution and subjected to reverse-phase HPLC purification using a preparative scale C$_{18}$ column and linear water–acetonitrile gradient elution. Fig. 3A shows a typical chromatogram obtained with UV detection at 280 nm, where TTR105–115 elutes at ~40 min. The identity and purity of recombinant TTR105–115 (MW ~ 1198 at natural abundance) were established by mass spectrometry as shown in Fig. 3B, and also by solution-state NMR spectroscopy as discussed below. The yield of purified peptide obtained by the procedure described above was ~4 mg per liter of minimal media culture (see Table 1). This result is an expected one given that the molecular weight of TTR105–115 is only ~13% of that for the His$_6$-GB1-TTR105–115 construct (i.e., ~4.5 mg would correspond to quantitative recovery of TTR105–115 for 35 mg of purified His$_6$-GB1-TTR105–115 starting material), and indicates that the expression level of fusion protein is the main factor that determines the ultimate yield of TTR105–115. While not pursued in the current study, it is possible that the yield of fusion protein per gram of ^{13}C-glucose/^{15}NH$_4$Cl could be further increased by the use of a fermentor.

Solution-state NMR characterization of TTR105–115

Solution-state NMR spectroscopy was used to further characterize recombinant TTR105–115. In Fig. 4 we compare 1D ^{1}H NMR spectra of a sample of HPLC-purified unlabeled recombinant TTR105–115 and a commercial TTR105–115 control sample prepared by Fmoc-SPPS. The similarity between the two spectra provides additional confirmation of the identity and purity of recombinant TTR105–115. 2D TOCSY and ROESY ^{1}H–^{1}H correlation spectra were acquired for both peptides to establish sequential resonance assignments (data not shown), and the observed ^{1}H chemical shifts were found to be in good agreement with previously published values [60]. Finally, to assess the efficiency of ^{13}C and ^{15}N isotopic labeling of recombinant TTR105–115 we recorded undecoupled and ^{15}N/^{13}C-decoupled 1D ^{1}H spectra, as well as 2D ^{1}H–^{15}N HSQC spectra, both ^{13}C-decoupled and ^{13}C′-coupled during ^{15}N evolution. The 2D datasets, shown in Fig. 5, indicate that uniform labeling is achieved for all residues as judged by the appear-

Table 1
Purification of TTR105–115 (1 L of minimal medium).

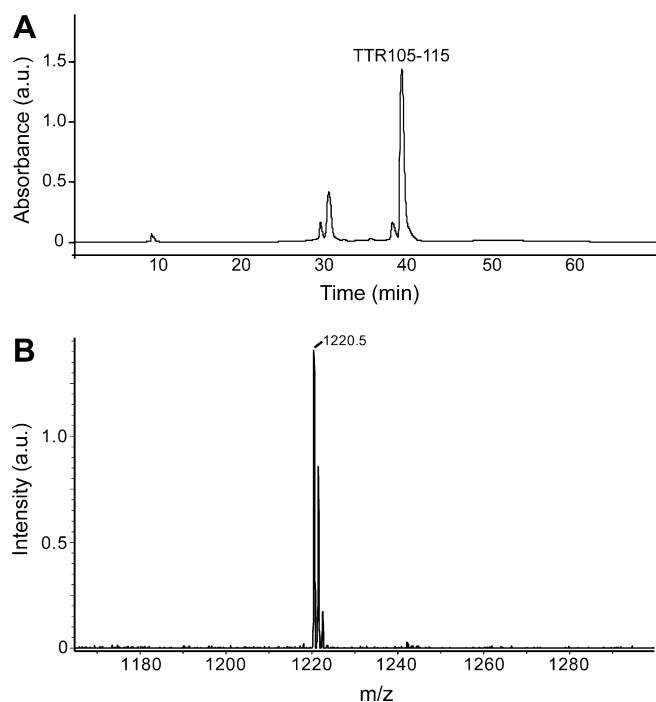| Purification step	Yield (mg)	Purity (%)
His$_6$-GB1-TTR105–115 cell lysate	~45	90
His$_6$-GB1-TTR105–115 after heating cell lysate at 80 °C	~40	95
His$_6$-GB1-TTR105–115 after Ni–NTA purification	32	98
TTR105–115 after cleavage and HPLC purification	3.8	99.9

Fig. 3. (A) Reverse-phase HPLC purification of a natural abundance recombinant TTR105–115 sample obtained from the Ni–NTA flow-through following Factor Xa digestion of His$_6$-GB1-TTR105–115. A preparative scale C$_{18}$ column was used and the sample was eluted with a linear acetonitrile gradient (3–90%) in water, containing 0.1% TFA; eluting fractions were monitored by UV absorbance at 280 nm. (B) MALDI TOF mass spectrum of the TTR105–115 fraction (peak at ~40 min in the chromatogram shown in panel A). The observed mass of 1220.5 Da corresponds to the sodium adduct of TTR105–115 (1198.3 + 22 Da).

Fig. 5. (A) Decoupled and (B) ^{13}C′-coupled 600 MHz ^{1}H–^{15}N HSQC spectra of recombinant U–^{13}C,^{15}N-labeled TTR105–115. Spectra were recorded as 256* (t_1, ^{15}N) × 700* (t_2, ^{1}H) data matrices with acquisition times of 178.5 ms (t_1) and 72.8 ms (t_2). The sample contained ~4 mM peptide in 20% acetonitrile-d_3, 0.1% TFA, and NMR data were collected at 25 °C. Resonance assignments are based on 2D ^{1}H–^{1}H TOCSY and ROESY spectra.

ance in the ^{13}C′-coupled HSQC spectrum (Fig. 5B) of characteristic E.COSY patterns [67] displaying ^{1}J$_{NC'}$ and ^{2}J$_{H^NC'}$ splittings in the ^{15}N and ^{1}H dimensions, respectively; mass spectra of recombinant

U–^{13}C,^{15}N TTR105–115 samples (data not shown) further confirm the quantitative ^{13}C and ^{15}N labeling of all peptide sites.

Electron microscopy and solid-state NMR spectroscopy of TTR105–115 amyloid fibrils

Amyloid fibrils were prepared by incubating TTR105–115 at 10 mg/mL in a 10% acetonitrile, pH 2, solution. We found that re-
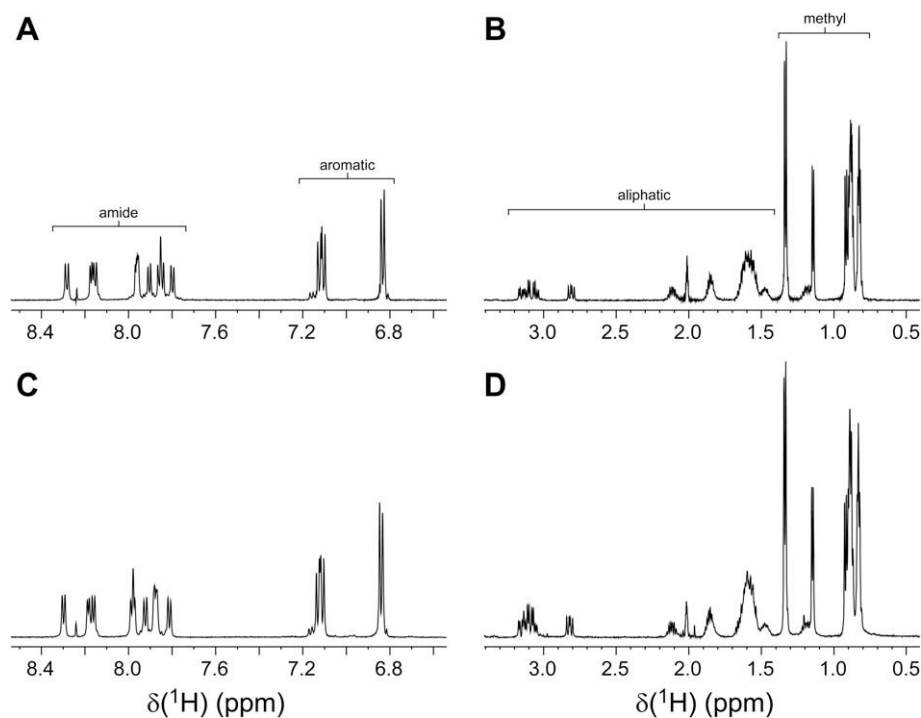

Fig. 4. Six-hundred MHz ^{1}H spectra of unlabeled TTR105–115 prepared using solid-phase peptide synthesis (A and B) and recombinant TTR105–115 (C and D), showing the amide/aromatic (A and C) and aliphatic (B and D) regions. Samples contained ~1 mM peptide in 20% acetonitrile-d_3, 0.1% TFA. Spectra were recorded at 25 °C.

combinant TTR105–115 formed amyloid fibrils as readily as the synthetic control sample, and in Fig. 6 we compare the electron micrographs of recombinant and synthetic TTR105–115 fibrils. Apart from minor differences in staining and local density of amyloid fibrils on the TEM grid, both peptides self-assemble into long, unbranched fibrils of ~10 nm in diameter. Most importantly, solid-state NMR spectroscopy confirms that recombinant and synthetic TTR105–115 fibrils are essentially identical on the molecular level. In Fig. 7 we show 1D ^{13}C cross-polarization MAS (CP-MAS), and 2D ^{13}C–^{13}C correlation spectra of amyloid fibrils formed from U–^{13}C,^{15}N-labeled recombinant TTR105–115. The spectra display ^{13}C linewidths of less than 1 ppm for most resonances—a quantita-
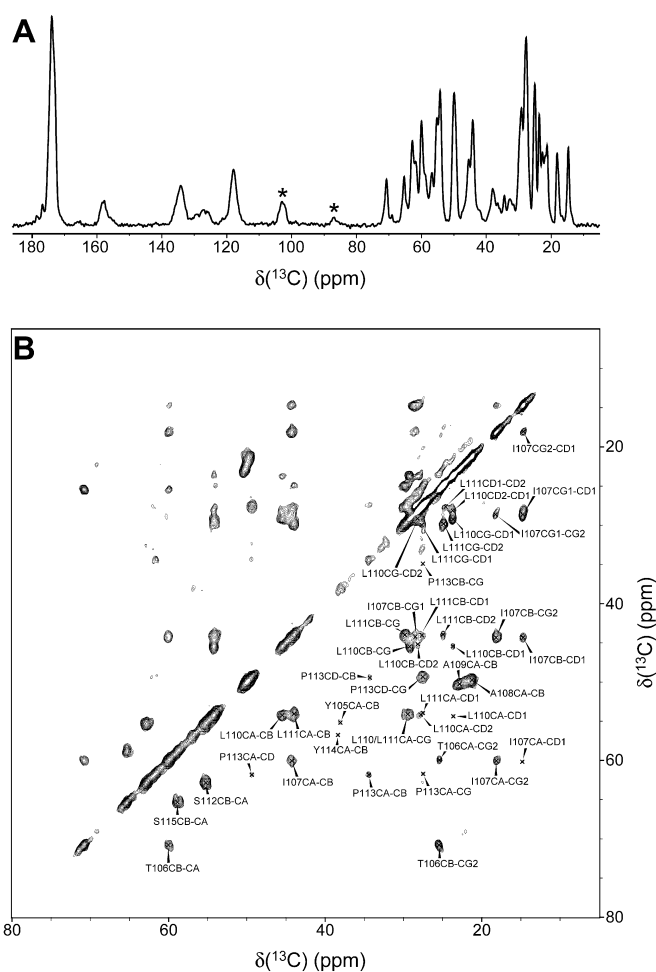
Fig. 7. Five-hundred MHz solid-state NMR spectra of U–^{13}C,^{15}N-labeled TTR105–115 amyloid fibrils recorded at ~5 °C and 8.929 kHz MAS. (A) 1D ^{13}C CP-MAS spectrum recorded with 1024 scans. Spinning sidebands are indicated by asterisks. (B) Aliphatic region of a 2D ^{13}C–^{13}C DARR correlation spectrum [68] acquired with 10 ms of mixing. The spectrum was recorded as a 640 (t_1) × 1000* (t_2) data matrix with acquisition times of 9 ms (t_1) and 20 ms (t_2), and total experiment time of 36 h. The resonance assignments are indicated.

tive determination yielded an average of 0.8 ± 0.2 ppm for a subset of 23 aliphatic ^{13}C signals in the 2D ^{13}C–^{13}C spectrum—indicating a high degree of order for individual TTR105–115 molecules within the fibril lattice [17,18]. Moreover, the ^{13}C chemical shifts for the U–^{13}C,^{15}N-labeled recombinant peptide prepared in this study could be readily mapped onto those previously reported for selectively ^{13}C,^{15}N-labeled synthetic TTR105–115 samples [17], with the average deviation of 0.1 ± 1.2 ppm for a set of 42 ^{13}C shifts.

Conclusions

We have described the expression and purification of a model 11 amino acid amyloidogenic peptide corresponding to residues 105–115 of human transthyretin. This recombinant TTR105–115 peptide contains no non-native residues, and was prepared as part of a fusion protein construct with a small, soluble GB1 domain containing an N-terminal 6× His-tag. Typical yields of U–^{13}C,^{15}N-enriched His$_6$-GB1-TTR105–115 fusion protein were approximately 40 mg per liter of minimal media culture, which translates into ~4 mg/L yields for HPLC-purified U–^{13}C,^{15}N TTR105–115. Thus a sample of U–^{13}C,^{15}N-TTR105–115 amyloid for solid-state NMR analysis can be readily obtained from a 1–2 L culture for a fraction of the cost and effort of an equivalent synthetic sample. Moreover,
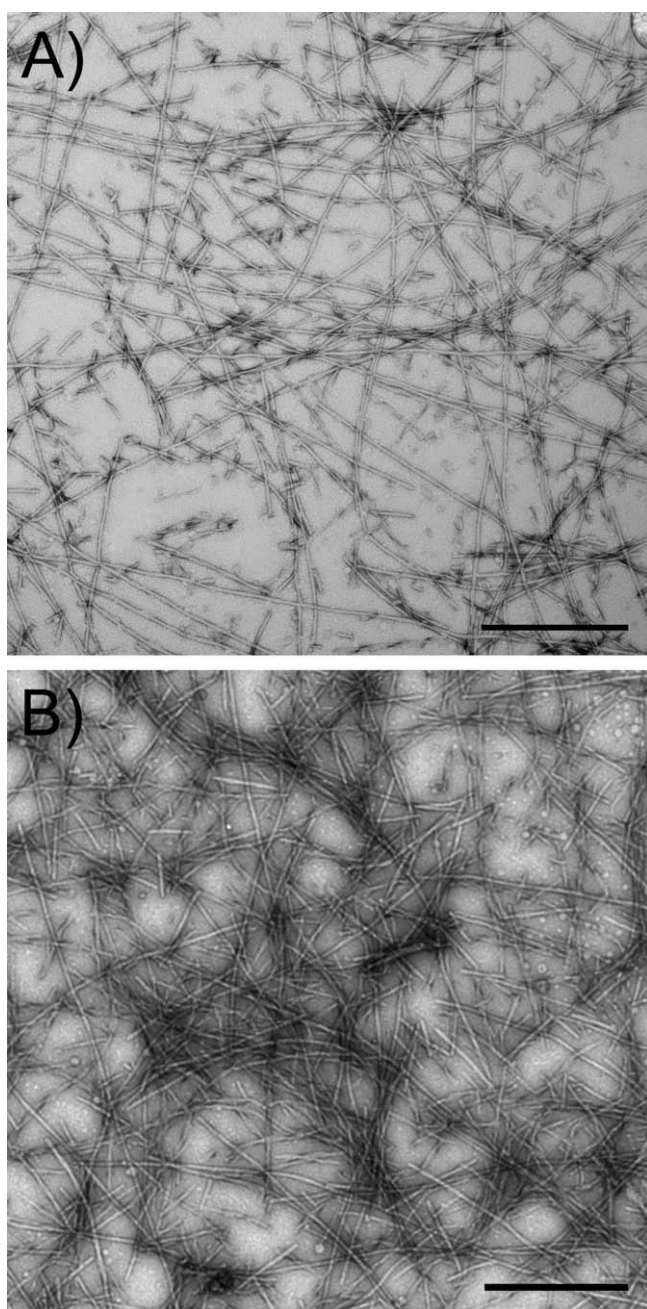

Fig. 6. Electron micrographs of (A) synthetic and (B) recombinant TTR105–115 amyloid fibrils. Fibrils were diluted to 1 mg/mL, negatively stained using 2% (w/v) uranyl acetate, and viewed using a FEI Technai G2 Spirit transmission electron microscope with an accelerating voltage of 80 kV. The scale bars correspond to 500 nm.

the ability to prepare TTR105–115 in this fashion enables the straightforward implementation of other isotopic labeling schemes such as sparse ^{13}C labeling or deuteration. Amyloid fibrils formed by recombinant TTR105–115 were characterized by electron microscopy and solid-state NMR spectroscopy, and found to be comparable to synthetic TTR105–115 fibrils. These results establish recombinant TTR105–115 as a valuable model system for the development of novel SSNMR methodologies for the characterization of amyloid structure with atomic-resolution.

Acknowledgments

References

[1] M. Sunde, C.C.F. Blake, From the globular to the fibrous state: protein structure and structural conversion in amyloid formation, Q. Rev. Biophys. 31 (1998) 1–39.
[2] J.W. Kelly, The alternative conformations of amyloidogenic proteins and their multi-step assembly pathways, Curr. Opin. Struct. Biol. 8 (1998) 101–106.
[3] C.M. Dobson, Protein misfolding, evolution and disease, Trends Biochem. Sci. 24 (1999).
[4] F. Chiti, C.M. Dobson, Protein misfolding, functional amyloid, and human disease, Annu. Rev. Biochem. 75 (2006) 333–366.
[5] J.I. Guijarro, M. Sunde, J.A. Jones, I.D. Campbell, C.M. Dobson, Amyloid fibril formation by an SH3 domain, Proc. Natl. Acad. Sci. USA 95 (1998) 4224–4228.
[6] M. Fändrich, M.A. Fletcher, C.M. Dobson, Amyloid fibrils from muscle myoglobin, Nature 410 (2001) 165–166.
[7] D.M. Fowler, A.V. Koulov, W.E. Balch, J.W. Kelly, Functional amyloid – from bacteria to humans, Trends Biochem. Sci. 32 (2007) 217–224.
[8] S. Zhang, Fabrication of novel biomaterials through molecular self-assembly, Nat. Biotechnol. 21 (2003) 1171–1178.
[9] C.E. MacPhee, D.N. Woolfson, Engineered and designed peptide-based fibrous biomaterials, Curr. Opin. Solid St. Mat. Sci. 8 (2004) 141–149.
[10] K. Channon, C.E. MacPhee, Possibilities for 'smart' materials exploiting the self-assembly of polypeptides into fibrils, Soft Matter 4 (2008) 647–652.
[11] R. Nelson, M.R. Sawaya, M. Balbirnie, A.O. Madsen, C. Riekel, R. Grothe, D. Eisenberg, Structure of the cross-b spine of amyloid-like fibrils, Nature 435 (2005) 747–749.
[12] M.R. Sawaya, S. Sambashivan, R. Nelson, M.I. Ivanova, S.A. Sievers, M.I. Apostol, M.J. Thompson, M. Balbirnie, J.J. Wiltzius, H.T. McFarlane, A.Ø. Madsen, C. Riekel, D. Eisenberg, Atomic structures of amyloid cross-b spines reveal varied steric zippers, Nature 447 (2007) 453–457.
[13] O.S. Makin, E. Atkins, P. Sikorski, J. Johansson, L.C. Serpell, Molecular basis for amyloid fibril formation and stability, Proc. Natl. Acad. Sci. USA 102 (2005) 315–320.
[14] P.T. Lansbury, P.R. Costa, J.M. Griffiths, E.J. Simon, M. Auger, K.J. Halverson, D.A. Kocisko, Z.S. Hendsch, T.T. Ashburn, R.G.S. Spencer, B. Tidor, R.G. Griffin, Structural model for the β-amyloid fibril based on interstrand alignment of an antiparallel-sheet comprising a C-terminal peptide, Nat. Struct. Biol. 2 (1995) 990–998.
[15] T.L.S. Benzinger, D.M. Gregory, T.S. Burkoth, H. Miller-Auer, D.G. Lynn, R.E. Botto, S.C. Meredith, Propagating structure of Alzheimer's b-amyloid(10–35) is parallel b-sheet with residues in exact register, Proc. Natl. Acad. Sci. USA 95 (1998) 13407–13412.
[16] A.T. Petkova, Y. Ishii, J.J. Balbach, O.N. Antzutkin, R.D. Leapman, F. Delaglio, R. Tycko, A structural model for Alzheimer's b-amyloid fibrils based on experimental constraints from solid-state NMR, Proc. Natl. Acad. Sci. USA 99 (2002) 16742–16747.
[17] C.P. Jaroniec, C.E. MacPhee, N.S. Astrof, C.M. Dobson, R.G. Griffin, Molecular conformation of a peptide fragment of transthyretin in an amyloid fibril, Proc. Natl. Acad. Sci. USA 99 (2002) 16748–16753.
[18] C.P. Jaroniec, C.E. MacPhee, V.S. Bajaj, M.T. McMahon, C.M. Dobson, R.G. Griffin, High-resolution molecular structure of a peptide in an amyloid fibril determined by magic angle spinning NMR spectroscopy, Proc. Natl. Acad. Sci. USA 101 (2004) 711–716.
[19] J.C.C. Chan, N.A. Oyler, W.M. Yau, R. Tycko, Parallel beta-sheets and polar zippers in amyloid fibrils formed by residues 10–39 of the yeast prion protein Ure2p, Biochemistry 44 (2005) 10669–10680.
[20] P.C.A. van der Wel, J.R. Lewandowski, R.G. Griffin, Solid-state NMR study of amyloid nanocrystals and fibrils formed by the peptide GNNQQNY from yeast prion protein Sup35p, J. Am. Chem. Soc. 129 (2007) 5117–5130.
[21] S. Luca, W.M. Yau, R. Leapman, R. Tycko, Peptide conformation and supramolecular organization in amylin fibrils: constraints from solid-state NMR, Biochemistry 46 (2007) 13505–13522.
[22] S.W. Lee, Y. Mou, S.Y. Lin, F.C. Chou, W.H. Tseng, C.H. Chen, C.Y. Lu, S.S. Yu, J.C.C. Chan, Steric zipper of the amyloid fibrils formed by residues 109–122 of the Syrian hamster prion protein, J. Mol. Biol. 378 (2008) 1142–1154.
[23] J. Madine, E. Jack, P.G. Stockley, S.E. Radford, L.C. Serpell, D.A. Middleton, Structural insights into the polymorphism of amyloid fibrils formed by region 20–29 of amylin revealed by solid-state NMR and X-ray fiber diffraction, J. Am. Chem. Soc. 130 (2008) 14990–15001.
[24] P. Walsh, K. Simonetti, S. Sharpe, Core structure of amyloid fibrils formed by residues 106–126 of the human prion protein, Structure 17 (2009) 417–426.
[25] F. Shewmaker, R.B. Wickner, R. Tycko, Amyloid of the prion domain of Sup35p has an in-register parallel b-sheet structure, Proc. Natl. Acad. Sci. USA 103 (2006) 19754–19759.
[26] U. Baxa, R.B. Wickner, A.C. Steven, D.E. Anderson, L.N. Marekov, W.M. Yau, R. Tycko, Characterization of b-sheet structure in Ure2p1–89 yeast prion fibrils by solid-state nuclear magnetic resonance, Biochemistry 46 (2007) 13149–13162.
[27] K. Iwata, T. Fujiwara, Y. Matsuki, H. Akutsu, S. Takahashi, H. Naiki, Y. Goto, 3D structure of amyloid protofilaments of b2-microglobulin fragment probed by solid-state NMR, Proc. Natl. Acad. Sci. USA 103 (2006) 18119–18124.
[28] N. Ferguson, J. Becker, H. Tidow, S. Tremmel, T.D. Sharpe, G. Krause, J. Flinders, M. Petrovich, J. Berriman, H. Oschkinat, A.R. Fersht, General structural motifs of amyloid protofilaments, Proc. Natl. Acad. Sci. USA 103 (2006) 16248–16253.
[29] H. Heise, W. Hoyer, S. Becker, O.C. Andronesi, D. Riedel, M. Baldus, Molecular-level secondary structure, polymorphism, and dynamics of full-length a-synuclein fibrils studied by solid-state NMR, Proc. Natl. Acad. Sci. USA 102 (2005) 15871–15876.
[30] K.D. Kloepper, D.H. Zhou, Y. Li, K.A. Winter, J.M. George, C.M. Rienstra, Temperature-dependent sensitivity enhancement of solid-state NMR spectra of a-synuclein fibrils, J. Biomol. NMR 39 (2007) 197–211.
[31] A.B. Siemer, C. Ritter, M. Ernst, R. Riek, B.H. Meier, High-resolution solid-state NMR spectroscopy of the prion protein HET-s in its amyloid conformation, Angew. Chem. Int. Ed. 44 (2005) 2441–2444.
[32] C. Wasmer, A. Lange, H. Van Melckebeke, A.B. Siemer, R. Riek, B.H. Meier, Amyloid fibrils of the HET-s(218–289) prion form a b solenoid with a triangular hydrophobic core, Science 319 (2008) 1523–1526.
[33] J.J. Helmus, K. Surewicz, P.S. Nadaud, W.K. Surewicz, C.P. Jaroniec, Molecular conformation and dynamics of the Y145Stop variant of human prion protein in amyloid fibrils, Proc. Natl. Acad. Sci. USA 105 (2008) 6284–6289.
[34] A.E. McDermott, Structural and dynamic studies of proteins by solid-state NMR spectroscopy: rapid movement forward, Curr. Opin. Struct. Biol. 14 (2004) 554–561.
[35] C.E. Hughes, M. Baldus, Magic-angle spinning solid-state NMR applied to polypeptides and proteins, Annu. Rep. NMR Spectrosc. 55 (2005) 121–158.
[36] A. Bockmann, 3D protein structures by solid-state NMR spectroscopy: ready for high resolution, Angew. Chem. Int. Ed. 47 (2008) 6110–6113.
[37] A. McDermott, Structure and dynamics of membrane proteins by magic angle spinning solid-state NMR, Annu. Rev. Biophys. 38 (2009) 385–403.
[38] D.M. LeMaster, D.M. Kushlan, Dynamical mapping of E. coli thioredoxin via ^{13}C NMR relaxation analysis, J. Am. Chem. Soc. 118 (1996) 9255–9264.
[39] H. Döbeli, N. Draeger, G. Huber, P. Jakob, D. Schmidt, B. Seilheimer, D. Stüber, B. Wipf, M. Zulauf, A biotechnological method provides access to aggregation competent monomeric Alzheimer's 1–42 residue amyloid peptide, Biotechnology 13 (1995) 988–993.
[40] M. Krampert, J. Bernhagen, J. Schmucker, A. Horn, A. Schmauder, H. Brunner, W. Voelter, A. Kapurniotu, Amyloidogenicity of recombinant human pro-islet amyloid polypeptide (ProIAPP), Chem. Biol. 7 (2000) 855–871.
[41] Y. Mazor, S. Gilead, I. Benhar, E. Gazit, Identification and characterization of a novel molecular-recognition and self-assembly domain within the islet amyloid polypeptide, J. Mol. Biol. 322 (2002) 1013–1024.
[42] D.H.J. Lopes, C. Colin, T.L. Degaki, A.V. de Sousa, M.N.N. Vieira, A. Sebollela, A.M. Blanco Martinez, C. Bloch Jr., S.T. Ferreira, M.C. Sogayar, Amyloidogenicity and cytotoxicity of recombinant mature human islet amyloid polypeptide (rhIAPP), J. Biol. Chem. 279 (2004) 42803–42810.
[43] M. Bisaglia, A. Trolio, I. Tessari, L. Bubacco, S. Mammi, E. Bergantino, Cloning, expression, purification, and spectroscopic analysis of the fragment 57–102 of human a-synuclein, Protein Expr. Purif. 39 (2005) 90–96.
[44] S. Sharpe, W.M. Yau, R. Tycko, Expression and purification of a recombinant peptide from the Alzheimer's β-amyloid protein for solid-state NMR, Protein Expr. Purif. 42 (2005) 200–210.
[45] E.K. Lee, J.H. Hwang, D.Y. Shin, D.I. Kim, Y.J. Yoo, Production of recombinant amyloid-β peptide 42 as an ubiquitin extension, Protein Expr. Purif. 40 (2005) 183–189.
[46] K. Wiesehan, S.A. Funke, M. Fries, D. Willbold, Purification of recombinantly expressed and cytotoxic human amyloid-β peptide 1–42, J. Chromatogr. B 856 (2007) 229–233.
[47] M. Nagata-Uchiyama, M. Yaguchi, Y. Hirano, T. Ueda, Expression and purification of uniformly ^{15}N-labeled amyloid b peptide 1–40 in Escherichia coli, Protein Pept. Lett. 14 (2007) 788–792.
[48] D.M. Walsh, E. Thulin, A.M. Minogue, N. Gustavsson, E. Pang, D.B. Teplow, S. Linse, A facile method for expression and purification of the Alzheimer's disease-associated amyloid β-peptide, FEBS J. 276 (2009) 1266–1281.
[49] A. Gustavsson, U. Engstrom, P. Westermark, Normal transthyretin and synthetic fragments form amyloid-like fibrils in vitro, Biochem. Biophys. Res. Commun. 175 (1991) 1159–1164.

[50] A. Kuliopulos, C.T. Walsh, Production, purification, and cleavage of tandem repeats of recombinant peptides, J. Am. Chem. Soc. 116 (1994) 4599–4607.

[51] P.T.F. Williamson, J.F. Roth, T. Haddingham, A. Watts, Expression and purification of recombinant neurotensin in *Escherichia coli*, Protein Expr. Purif. 19 (2000) 271–275.

[52] B.W. Koenig, M. Rogowski, J.M. Louis, A rapid method to attain isotope labeled small soluble peptides for NMR studies, J. Biomol. NMR 26 (2003) 193–202.

[53] D.A. Lindhout, A. Thiessen, D. Schieve, B.D. Sykes, High-yield expression of isotopically labeled peptides for use in NMR studies, Protein Sci. 12 (2003) 1786–1791.

[54] J.R. Huth, C.A. Bewley, B.M. Jackson, A.G. Hinnebusch, G.M. Clore, A.M. Gronenborn, Design of an expression system for detecting folded protein domains and mapping macromolecular interactions by NMR, Protein Sci. 6 (1997) 2359–2364.

[55] P. Zhou, A.A. Lugovskoy, G. Wagner, A solubility-enhancement tag (SET) for NMR studies of poorly behaving proteins, J. Biomol. NMR 20 (2001) 11–14.

[56] Y. Cheng, D.J. Patel, An efficient system for small protein expression and refolding, Biochem. Biophys. Res. Commun. 317 (2004) 401–405.

[57] W.J. Bao, Y.G. Gao, Y.G. Chang, T.Y. Zhang, X.J. Lin, X.Z. Yan, H.Y. Hu, Highly efficient expression and purification system of small-size protein domains in *Escherichia coli* for biochemical characterization, Protein Expr. Purif. 47 (2006) 599–606.

[58] M.L. Cai, Y. Huang, K. Sakaguchi, G.M. Clore, A.M. Gronenborn, R. Craigie, An efficient and cost-effective isotope labeling protocol for proteins expressed in *Escherichia coli*, J. Biomol. NMR 11 (1998) 97–102.

[59] J. Cavanagh, W.J. Fairbrother, A.G. Palmer, M. Rance, N.J. Skelton, Protein NMR Spectroscopy: Principles and Practice, Elsevier Academic Press, San Diego, CA, 2007.

[60] J.A. Jarvis, A. Kirkpatrick, D.J. Craik, ^{1}H NMR analysis of fibril-forming peptide fragments of transthyretin, Int. J. Peptide Protein Res. 44 (1994) 388–398.

[61] F. Delaglio, S. Grzesiek, G.W. Vuister, G. Zhu, J. Pfeifer, A. Bax, NMRPipe: a multidimensional spectral processing system based on UNIX pipes, J. Biomol. NMR 6 (1995) 277–293.

[62] T.D. Goddard, D.G. Kneller, SPARKY 3, University of California, San Francisco, 1993.

[63] J.A. Stringer, C.E. Bronnimann, C.G. Mullen, D.H.H. Zhou, S.A. Stellfox, Y. Li, E.H. Williams, C.M. Rienstra, Reduction of RF-induced sample heating with a scroll coil resonator structure for solid-state NMR probes, J. Magn. Reson. 173 (2005) 40–48.

[64] A.E. Bennett, C.M. Rienstra, M. Auger, K.V. Lakshmi, R.G. Griffin, Heteronuclear decoupling in rotating solids, J. Chem. Phys. 103 (1995) 6951–6957.

[65] C.R. Morcombe, K.W. Zilm, Chemical shift referencing in MAS solid state NMR, J. Magn. Reson. 162 (2003) 479–486.

[66] A.M. Gronenborn, D.R. Filpula, N.Z. Essig, A. Achari, M. Whitlow, P.T. Wingfield, G.M. Clore, A novel, highly stable form of the immunoglobulin binding domain of streptococcal protein G, Science 253 (1991) 657–661.

[67] C. Griesinger, O.W. Sørensen, R.R. Ernst, Two-dimensional correlation of connected NMR transitions, J. Am. Chem. Soc. 107 (1985) 6394–6396.

[68] K. Takegoshi, S. Nakamura, T. Terao, ^{13}C–^{1}H dipolar-assisted rotational resonance in magic-angle spinning NMR, Chem. Phys. Lett. 344 (2001) 631–637.